CLNS 10/2067
CLEO 10-4

Studies of $D^+ \to \{\eta', \eta, \phi\} e^+ \nu_e$

J. Yelton,[1] P. Rubin,[2] N. Lowrey,[3] S. Mehrabyan,[3] M. Selen,[3] J. Wiss,[3] M. Kornicer,[4] R. E. Mitchell,[4] M. R. Shepherd,[4] C. M. Tarbert,[4] D. Besson,[5] T. K. Pedlar,[6] J. Xavier,[6] D. Cronin-Hennessy,[7] J. Hietala,[7] P. Zweber,[7] S. Dobbs,[8] Z. Metreveli,[8] K. K. Seth,[8] A. Tomaradze,[8] T. Xiao,[8] S. Brisbane,[9] J. Libby,[9] L. Martin,[9] A. Powell,[9] P. Spradlin,[9] G. Wilkinson,[9] H. Mendez,[10] J. Y. Ge,[11] D. H. Miller,[11] I. P. J. Shipsey,[11] B. Xin,[11] G. S. Adams,[12] D. Hu,[12] B. Moziak,[12] J. Napolitano,[12] K. M. Ecklund,[13] J. Insler,[14] H. Muramatsu,[14] C. S. Park,[14] L. J. Pearson,[14] E. H. Thorndike,[14] F. Yang,[14] S. Ricciardi,[15] C. Thomas,[16] M. Artuso,[16] S. Blusk,[16] R. Mountain,[16] T. Skwarnicki,[16] S. Stone,[16] J. C. Wang,[16] L. M. Zhang,[16] G. Bonvicini,[17] D. Cinabro,[17] A. Lincoln,[17] M. J. Smith,[17] P. Zhou,[17] J. Zhu,[17] P. Naik,[18] J. Rademacker,[18] D. M. Asner,[19,*] K. W. Edwards,[19] K. Randrianarivony,[19] G. Tatishvili,[19,*] R. A. Briere,[20] H. Vogel,[20] P. U. E. Onyisi,[21] J. L. Rosner,[21] J. P. Alexander,[22] D. G. Cassel,[22] S. Das,[22] R. Ehrlich,[22] L. Fields,[22] L. Gibbons,[22] S. W. Gray,[22] D. L. Hartill,[22] B. K. Heltsley,[22] D. L. Kreinick,[22] V. E. Kuznetsov,[22] J. R. Patterson,[22] D. Peterson,[22] D. Riley,[22] A. Ryd,[22] A. J. Sadoff,[22] X. Shi,[22] and W. M. Sun[22]

[1] *University of Florida, Gainesville, Florida 32611, USA*
[2] *George Mason University, Fairfax, Virginia 22030, USA*
[3] *University of Illinois, Urbana-Champaign, Illinois 61801, USA*
[4] *Indiana University, Bloomington, Indiana 47405, USA*
[5] *University of Kansas, Lawrence, Kansas 66045, USA*
[6] *Luther College, Decorah, Iowa 52101, USA*
[7] *University of Minnesota, Minneapolis, Minnesota 55455, USA*
[8] *Northwestern University, Evanston, Illinois 60208, USA*
[9] *University of Oxford, Oxford OX1 3RH, UK*
[10] *University of Puerto Rico, Mayaguez, Puerto Rico 00681*
[11] *Purdue University, West Lafayette, Indiana 47907, USA*
[12] *Rensselaer Polytechnic Institute, Troy, New York 12180, USA*
[13] *Rice University, Houston, Texas 77005, USA*
[14] *University of Rochester, Rochester, New York 14627, USA*
[15] *STFC Rutherford Appleton Laboratory, Chilton, Didcot, Oxfordshire, OX11 0QX, UK*
[16] *Syracuse University, Syracuse, New York 13244, USA*
[17] *Wayne State University, Detroit, Michigan 48202, USA*
[18] *University of Bristol, Bristol BS8 1TL, UK*
[19] *Carleton University, Ottawa, Ontario, Canada K1S 5B6*
[20] *Carnegie Mellon University, Pittsburgh, Pennsylvania 15213, USA*
[21] *University of Chicago, Chicago, Illinois 60637, USA*
[22] *Cornell University, Ithaca, New York 14853, USA*

(Dated: November 4, 2010)

Abstract

We report the first observation of the decay $D^+ \to \eta' e^+ \nu_e$ in two analyses with significances of 5.6 (total) and 5.8 (statistical) standard deviations. These analyses also provide the first form factor measurement and the most precise branching fraction measurement for $D^+ \to \eta e^+ \nu_e$. We also improve the upper limit for $D^+ \to \phi\, e^+ \nu_e$.

*Now at: Pacific Northwest National Laboratory, Richland, WA 99352

Semileptonic decay provides an excellent laboratory for the study of both weak and strong interactions. Charm semileptonic decay allows determination of the parameters $|V_{cd}|$ and $|V_{cs}|$ from the Cabibbo-Kobayashi-Maskawa (CKM) matrix [1], and stringent testing of predictions for QCD contributions to the decay amplitude. A complete understanding of charm semileptonic decay requires study of both high-statistics and rare modes.

The semileptonic decay $D^+ \to \eta' e^+ \nu_e$ has not yet been observed. Its rate relative to $D^+ \to \eta e^+ \nu_e$ will provide information about $\eta - \eta'$ mixing [2], as well as about the role of the QCD anomaly in heavy quark decays involving η' [3]. Study of these modes also probes the composition of the η and η' wave functions when combined with measurements of the corresponding D_s semileptonic decay modes [4], and can gauge the possible role of weak annihilation in the corresponding D_s-meson semileptonic decays. The process $D^+ \to \phi\, e^+ \nu_e$ is not expected to occur in the absence of mixing between the ω and ϕ.

The differential decay rate for $D^+ \to \eta e^+ \nu_e$ is given, in the limit of negligible electron mass, by

$$\frac{d\Gamma}{dq^2} = \frac{G_F^2 |V_{cd}|^2 |\mathbf{p}_\eta|^3}{24\pi^3} |f_+(q^2)|^2, \tag{1}$$

where G_F is the Fermi constant, V_{cd} is the CKM matrix element for $c \to d$ transitions, and $\mathbf{p}_\eta$ is the η momentum in the D rest frame. The form factor $f_+(q^2)$ parameterizes the strong interaction dynamics as a function of the hadronic four-momentum transfer q^2. Measurement of $d\Gamma/dq^2$ probes $f_+(q^2)$ and the QCD dynamics needed to determine many CKM matrix elements.

We report herein the first observation of $D^+ \to \eta' e^+ \nu_e$, an improved $\mathcal{B}(D^+ \to \eta e^+ \nu_e)$ and first $f_+(q^2)$ study, and a search for $D^+ \to \phi\, e^+ \nu_e$ (charge-conjugate modes implied). The results derive from two analyses of 818 pb^{-1} of e^+e^- collision data (2.4×10^6 D^+D^- pairs) collected with the CLEO-c detector [5] at the $\psi(3770)$ resonance.

One analysis employs the tagging technique used in past CLEO-c studies of these [6] and other [7] semileptonic modes. A parent event sample is defined by reconstruction of either D meson in a specific (tag) hadronic decay mode. The fraction of these events in which the other D is reconstructed in the signal semileptonic mode determines the absolute semileptonic branching fraction $\mathcal{B}_{\rm SL} = (N_{\rm tag,SL}/N_{\rm tag})(\epsilon_{\rm tag}/\epsilon_{\rm tag,SL})$. Here $N_{\rm tag}$ and $\epsilon_{\rm tag}$ are the yield and reconstruction efficiency, respectively, for the hadronic tag, and $N_{\rm tag,SL}$ and $\epsilon_{\rm tag,SL}$ are those for the combined semileptonic decay and hadronic tag [6].

The six tag modes $K^+\pi^-\pi^-$, $K^+\pi^-\pi^-\pi^0$, $K^0_S\pi^-$, $K^0_S\pi^-\pi^0$, $K^0_S\pi^-\pi^-\pi^+$, and $K^+K^-\pi^-$ are selected based on the difference in energy $\Delta E \equiv E_D - E_{\rm beam}$ of the D tag candidate (E_D) and the beam ($E_{\rm beam}$), and on the beam-constrained mass $M_{\rm BC} \equiv \sqrt{E^2_{\rm beam}/c^4 - |\mathbf{p}_D|^2/c^2}$, where $\mathbf{p}_D$ is the reconstructed momentum of the D candidate. Reference [8] summarizes the selection criteria and their performance for the $\pi^\pm$, $K^\pm$, π^0 and K^0_S candidates. From multiple candidates of the same mode and charge, we choose that with the smallest $|\Delta E|$. The yield of each tag mode is obtained from a fit [8] to its $M_{\rm BC}$ distribution. We find a total of 481223$\pm$809 $D^\pm$ tags.

We search each tagged event for an $e^\pm$ and an η ($\gamma\gamma$ and $\pi^+\pi^-\pi^0$ modes), η' ($\pi^+\pi^-\eta$ mode), or ϕ (K^+K^- mode) candidate following Ref. [6]. Candidate $\pi^\pm e^\mp$ or $K^\pm e^\mp$ pairs must have an opening angle $\theta > 20^\circ$ to suppress γ conversion backgrounds. The combined tag and semileptonic candidates must account for all tracks in the event. The undetected neutrino leads to missing energy $E_{\rm miss} \equiv E_{\rm beam} - E_{h+e}$ and missing momentum $\mathbf{p}_{\rm miss} \equiv -[\mathbf{p}_{h+e} + \widehat{\mathbf{p}}_{\rm tag}\sqrt{(E_{\rm beam}/c)^2 - m_D^2 c^2}]$, where $E_{h+e} \equiv E_h + E_e$, $\mathbf{p}_{h+e} \equiv \mathbf{p}_h + \mathbf{p}_e$, and $\widehat{\mathbf{p}}_{\rm tag}$ is the unit vector

in the direction of the tag D^- momentum. Correctly reconstructed semileptonic candidates peak at zero in $U \equiv E_{\rm miss} - c|\mathbf{p}_{\rm miss}|$, which has a 10 MeV resolution. For each tag mode of a given charge in each event, we allow only one semileptonic candidate, taking that with the smallest $\sum_X \chi^2_M(X)$, where we sum over all reconstructed $X \in (\pi^0, \eta, \eta', \phi)$. The "pull" for particle X is $\chi_M(X) \equiv (M_{\rm r} - M_X)/\sigma_M$ where $M_{\rm r}$ and M_X are the reconstructed and nominal [9] masses, and the resolution σ_M derives from the error matrices of X's daughters.

The second analysis, generic reconstruction (GR) [10], refines techniques optimized for association of event-wide missing energy ($E^{\rm evt}_{\rm miss}$) and momentum ($\mathbf{p}^{\rm evt}_{\rm miss}$) with a neutrino [11]. We apply the track and photon selection algorithms of Reference [11], and impose the associated event-level criteria to reduce background from undetected particles: no net charge and only one identified $e^\pm$. We then search for η ($\gamma\gamma$, $\pi^+\pi^-\pi^0$ and $3\pi^0$ modes) and η' ($\pi^+\pi^-\eta$, $\pi^0\pi^0\eta_{\gamma\gamma}$, $\rho\gamma$ and $\gamma\gamma$ modes) candidates, using criteria [10] similar to those of the tagged analysis. For $\eta' \to \rho\gamma$, the $\pi^\pm$ and γ must have an opening angle $\theta_{\pi\gamma}$ in the ρ^0 rest frame satisfying $|\cos\theta_{\pi\gamma}| < 0.85$. Signal varies as $\sin^2\theta_{\pi\gamma}$; background is flat. For each $\eta^{(\prime)}e^\pm\nu_e$ candidate, the GR algorithm attempts reconstruction of a hadronic decay for the second D from the remaining particle content. Doing so improves the $E^{\rm evt}_{\rm miss}$ and $\mathbf{p}^{\rm evt}_{\rm miss}$ resolutions and suppresses combinatoric background.

We form two sets of selected tracks outside the semileptonic candidate: (i) non-overlapping $K^0_S \to \pi^+\pi^-$ candidates, and (ii) tracks consistent with the primary vertex. The K^0_S candidates must be within 12 MeV/c^2 of M_{K^0}, overlapping candidates are resolved using the best mass, and final candidates are kinematically fit with a mass constraint. A selected track outside of these categories is most likely a K^0_S daughter whose sibling was used in the semileptonic candidate, so that candidate is rejected.

To enhance photon candidate purity, we form a non-overlapping π^0 and η to $\gamma\gamma$ list, with overlaps resolved based on the smallest $|\chi_M(\pi^0)|$ and $|\chi_M(\eta)|$. High efficiency dictates the broad range $-25(-15) < \chi_M < 15$ for π^0 (η) candidates. Unpaired showers with energy below 100 MeV (250 MeV if $K^\pm$ are present) are likely hadronic shower remnants and are vetoed. The $\gamma\gamma$ candidates are refit with a mass constraint prior to use in reconstruction.

We form the π^0, η, K^0_S, and remaining photons and tracks into the non-signal D candidate. Combining this D with the signal $e^\pm$ and $\eta^{(\prime)}$ candidates gives $E^{\rm evt}_{\rm miss}$, $\mathbf{p}^{\rm evt}_{\rm miss}$, the signal D momentum $\mathbf{p}_{\rm sig}$, and its energy $E_{\rm sig}$. Charge correlations are enforced assuming Cabibbo-favored decays. We require $E^{\rm evt}_{\rm miss} > 50$ MeV and a total vetoed-shower energy under 300 MeV. ΔE for both D candidates and $E^{\rm evt}_{\rm miss} - c|\mathbf{p}^{\rm evt}_{\rm miss}|$ must be consistent with zero within mode-dependent resolutions of about 100 MeV. To improve resolution in $\Delta E_{\rm sig}$, we take $E_\nu = c|\mathbf{p}^{\rm evt}_{\rm miss}|$. We further improve $M_{\rm BC}$ by correcting $\mathbf{p}^{\rm evt}_{\rm miss}$ using the observed $\Delta E_{\rm sig}$: $\mathbf{p}_\nu = \zeta\mathbf{p}^{\rm evt}_{\rm miss}$ with $\zeta = 1 + \Delta E_{\rm sig}/(c|\mathbf{p}^{\rm evt}_{\rm miss}|)$. Signal mode yields are determined from fits to the $M_{\rm BC}$ distribution. To increase signal sensitivity in our yield fit, we classify a high-quality (HQ) sample with the following properties: no unused showers, all $\gamma\gamma$ candidates with $-5 < \chi_M(Y) < 3$, $Y \in (\eta, \pi^0)$, and a non-signal D satisfying the tagged analysis ΔE and $M_{\rm BC}$ criteria. Reconstruction efficiencies, not including submode branching fractions, range from 2–5% overall, and 1–3% for the HQ subsample.

To reduce the dominant background from more copious charm semileptonic modes, the GR $\eta' e^+\nu_e$ candidates must satisfy $\chi^2_M(D)_{\eta'} - \chi^2_M(D)_{\rm min} < 9$, where $\chi_M(D)_{\rm min}$ is the smallest magnitude non-signal D mass pull of all semileptonic candidates in an event. This requirement halves the background level with 90% signal efficiency.

Continuum backgrounds arise largely from γ conversions or π^0 Dalitz decays with one $e^\pm$ below identification threshold. The $e^\pm$ candidate is combined with each track t below

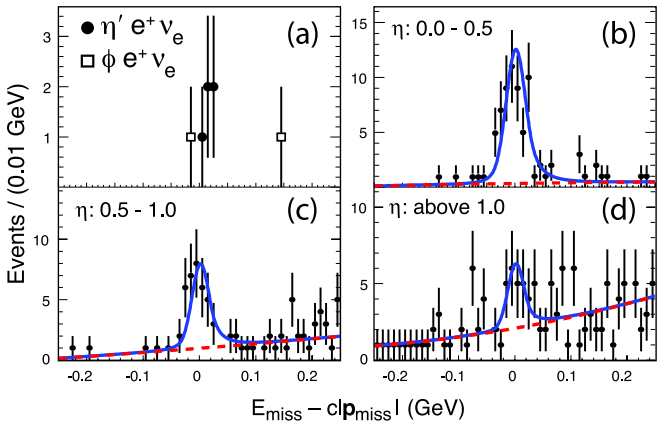

FIG. 1. Tagged U distributions for data (points) summed over all submodes. (a) $D^+ \to \{\eta', \phi\}e^+\nu_e$. (b–d) $\eta e^+\nu_e$ in the indicated q^2 [GeV$^2/c^4$] ranges, overlaid with the total (solid line) and background (dashed line) shapes from the fits.

the 200 MeV/c threshold but with dE/dx consistent with an $e^\mp$, and each pair with every photon. Rejecting events with any $m_{e^\pm t^\pm} < 100$ MeV/c^2 or $|m_{e^\pm t^\mp \gamma} - m_{\pi^0}| < 50$ MeV/c^2 eliminates this background.

The $\eta' e^+\nu_e$ yields are normalized to the $K^-\pi^+\pi^+$ yield determined using the GR technique, but with reversal of the $E^{\rm evt}_{\rm miss}$ requirement ($E^{\rm evt}_{\rm miss} < 100$ MeV) and imposition of a $|\chi_M(D)| < 3$ requirement on the non-signal D.

To find $q^2 = (p_{e^+} + p_{\nu_e})^2/c^2$, the tagged and GR analyses define the ν_e four momentum p_ν as $(E_{\rm miss}, E_{\rm miss}\hat{\mathbf{p}}_{\rm miss})$ and $\zeta(|\mathbf{p}^{\rm evt}_{\rm miss}|, \mathbf{p}^{\rm evt}_{\rm miss})$, respectively. The data are divided into the q^2 ranges $0-0.5$, $0.5-1.0$, and ≥ 1.0 GeV$^2/c^4$.

Efficiency and background determinations utilize a Monte Carlo (MC) simulation based on GEANT [12] for the detector and EvtGen [13] for the physics simulation. The analyses utilize a generic $D\bar{D}$ sample in which both D mesons decay according to the full model (34 times the data statistics), a non-$D\bar{D}$ sample that incorporates both continuum $e^+e^- \to q\bar{q}$ ($q = u, d$ or s) processes and radiative return production of $\psi(2S)$, and $e^+e^- \to \tau^+\tau^-$, as well as several specialized samples.

Figure 1 shows the U distributions for the tagged analysis. We observe no significant $D^+ \to \phi\, e^+\nu_e$ signal. We have five $D^+ \to \eta' e^+\nu_e$, $\eta' \to \pi^+\pi^-\eta$ candidates: four with $\eta \to \gamma\gamma$ and one with $\eta \to \pi^+\pi^-\pi^0$, with reconstruction efficiencies of 3.26(4)% and 0.86(2)%, respectively, including subsidiary branching fractions. MC studies predict a total background for the combined η' decay modes of 0.043 ± 0.026 events arising primarily from $D^+ \to \eta(\pi^+\pi^-\gamma)e^+\nu_e$, $D^+ \to \eta(\pi^+\pi^-\pi^0)e^+\nu_e$, and $D^+ \to \omega(\pi^+\pi^-\pi^0)e^+\nu_e$ with correctly identified tags. Using a toy simulation that folds Poisson statistics with statistical and systematic uncertainties, we find the probability for this background to fluctuate into 5 events to be 9.7×10^{-9}, a 5.6 standard deviation (s.d.) significance.

The $\eta e^+\nu_e$ yields come from binned likelihood fits to the U distributions in each submode. The Crystal Ball shape [14], with two power-law tails to account for initial- and final-state radiation (FSR) and mismeasured tracks, describes the signal. Signal and background normalizations float in the fits, with shapes fixed from fits to MC samples. The main backgrounds are misreconstructed semileptonic decays with correctly reconstructed tags.

The GR $M_{\rm BC}$ distributions for HQ and non-HQ samples from all η' and η submodes and

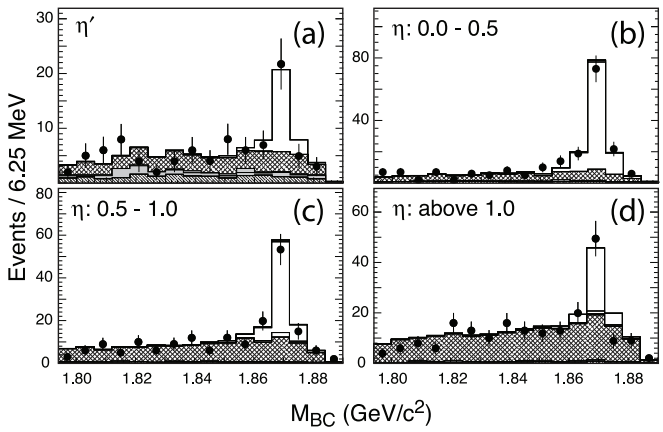

FIG. 2. $M_{\rm BC}$ distributions (GR analysis) for data (points) and signal (unshaded), $D\bar{D}$ (crosshatch), continuum (grey) and fake $e^{\pm}$ (45° hatch) fit components. (a) $\eta' e^+\nu_e$. (b–d) $\eta e^+\nu_e$ in the indicated q^2 [GeV$^2/c^4$] ranges.

q^2 intervals and from $K^-\pi^+\pi^+$ are fit simultaneously with reconstructed MC distributions. Simultaneous fitting accommodates crossfeed among all modes. Critical aspects of the signal and $D\bar{D}$ MC samples are first corrected using independent comparisons to data: the hadronic D decay model (108 modes probed), K^0_L and non-K^0_L hadronic showering in the calorimeter, π^0 and $\eta\to\gamma\gamma$ reconstruction efficiencies, and FSR. The $\eta' e^+\nu_e$ and three $\eta e^+\nu_e$ efficiency-corrected yields and the $D\bar{D}$ background normalization for each submode float in the fit. Figure 2 shows excellent agreement between data and fit projections. Fixing the $\eta' e^+\nu_e$ yield to zero increases the $-2\ln\mathcal{L}$ by +33.6, corresponding to a 5.8 s.d. statistical significance.

The systematic uncertainties in both analyses are dominated by uncertainties in the $\eta\to\gamma\gamma$ and $\pi^0\to\gamma\gamma$ detection efficiencies, with other common contributions including track finding efficiency, $e^{\pm}$, $K^{\pm}$ and $\pi^{\pm}$ identification, FSR and form-factor modeling. Other tagged contributions include uncertainties in $N_{\rm tag}$, the no-additional-track requirement and the signal U parameterization. The remaining GR uncertainties arise in the MC corrections described above. Many significant uncertainties (*e.g.* tracking efficiency and hadronic decay model) largely cancel in the $K^-\pi^+\pi^+$ normalization. To account for the systematic uncertainty in $\mathcal{B}(D^+\to\phi\, e^+\nu_e)$, we increase the upper limit by one standard deviation.

Table I summarizes all branching fraction results. Each GR branching fraction $\mathcal{B}_{\rm GR}$ was obtained from the ratio $R_{\rm GR}=\mathcal{B}(D^+\to\eta^{(\prime)}e^+\nu_e)/\mathcal{B}(D^+\to K^-\pi^+\pi^+)$ using $\mathcal{B}(D^+\to K^-\pi^+\pi^+)=(9.14\pm0.20)\%$ [8]. All results from the two techniques are consistent. They are also statistically and systematically correlated, and full correlation information is available from EPAPS [15].

To extract $f_+(q^2)$ for $D^+\to\eta e^+\nu_e$, we fit the partial rates obtained from our partial branching fractions using $\tau_{D^+}=1040(7)\times10^{-15}$s [9], minimizing $\chi^2=\Delta\gamma^T V^{-1}\Delta\gamma$. The array $\Delta\gamma=\Delta\Gamma_r-\Delta\Gamma_p$, where $\Delta\Gamma_r$ ($\Delta\Gamma_p$) holds the measured (predicted) partial widths, and V is the covariance matrix. We fit the two analyses simultaneously, accounting for statistical correlations within each analysis and sample overlap between analyses, as well as for systematic correlations. We fit first with the statistical ($V=V_{\rm stat}$) and then with the combined statistical and systematic ($V=V_{\rm stat}+V_{\rm syst}$) covariance.

We integrate Eq. 1 over each q^2 interval to predict $\Delta\Gamma_p$, with $f_+(q^2)\equiv(\sum_k a_k z(q^2,t_0)^k)/(P(q^2)\phi(q^2,t_0))$ (see Ref. [16]) truncated at $k=1$. We float $f_+(0)|V_{cd}|$ and $r_1=a_1/a_0$ in the fit, and find

TABLE I. Branching fractions from the tagged ($\mathcal{B}_{\rm tag}$) and GR ($\mathcal{B}_{\rm GR}$) analyses, and branching fraction ratios $R_{\rm GR}$ relative to $\mathcal{B}(D^+ \to K^-\pi^+\pi^+)$. Errors are statistical, then systematic.

Mode	$\mathcal{B}_{\rm tag}$ [10^{-4}]	$R_{\rm GR}$ [%]	$\mathcal{B}_{\rm GR}$ [10^{-4}]
$\eta' e^+\nu_e$	$2.5^{+1.6}_{-1.0}(0.1)$	0.237(58)(5)	2.16(53)(7)
$\phi\, e^+\nu_e$	< 0.9 @ 90% confidence level (C.L.)		
$\eta e^+\nu_e$	11.1(1.3)(0.4)	1.28(11)(4)	11.7(1.0)(0.4)
$\eta e^+\nu_{e,0-0.5}$	6.53(94)(26)	0.625(69)(18)	5.71(63)(20)
$\eta e^+\nu_{e,0.5-1.0}$	3.08(71)(13)	0.437(68)(13)	3.99(62)(15)
$\eta e^+\nu_{e,\geq 1.0}$	1.77(67)(16)	0.223(52)(10)	2.03(47)(10)

$f_+(0)|V_{cd}| = 0.086 \pm 0.006 \pm 0.001$ and $r_1 = -1.83 \pm 2.23 \pm 0.28$, with a correlation of $\rho = 0.81$. The fit has a $\chi^2 = 2.5$ for 4 degrees of freedom (see Fig. 3). With $|V_{cd}| = 0.2256 \pm 0.0010$ [9], $f_+(0) = 0.381 \pm 0.027 \pm 0.005$. EPAPS [15] has results for other $f_+(q^2)$ parameterizations. We obtain the total branching fraction by integrating the fit result.

In conclusion, our combined branching fraction results

$$\mathcal{B}(D^+ \to \eta e^+\nu_e) = (11.4 \pm 0.9 \pm 0.4) \times 10^{-4},$$
$$\mathcal{B}(D^+ \to \eta' e^+\nu_e) = (2.16 \pm 0.53 \pm 0.07) \times 10^{-4},$$
$$\mathcal{B}(D^+ \to \phi\, e^+\nu_e) < 0.9 \times 10^{-4} \quad (90\%\ \text{C.L.})$$

are consistent with our previous results [6], which they supersede, and with predictions from the ISGW2 [2] and Fajfer-Kamenic [17] models. The limit on $D^+ \to \phi\, e^+\nu_e$ is twice as restrictive as the previous best limits [6, 9].

We gratefully acknowledge the CESR staff for the excellent luminosity and running conditions, and the support of the A.P. Sloan Foundation, the National Science Foundation, the U.S. Department of Energy, the Natural Sciences and Engineering Research Council of Canada, and the U.K. Science and Technology Facilities Council.

[1] M. Kobayashi and T. Maskawa, Theor. Phys. **49**, 652 (1973); N. Cabibbo, Phys. Rev. Lett. **10**, 531 (1963).

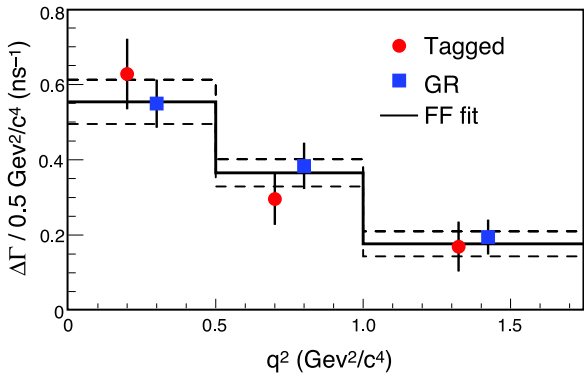

FIG. 3. The partial rates from the tagged (circles) and GR (squares) analyses, and the form factor (FF) fit (histogram). The dashed lines indicate the total uncertainty on the fit rates.

[2] D. Scora and N. Isgur, Phys. Rev. D **52**, 2783 (1995).
[3] T. Feldmann, P. Kroll and B. Stech, Phys. Rev. D **58**, 114006 (1998).
[4] S. Bianco, F. Fabbri, D. Benson, and I. Bigi, La Rivista del Nuovo Cimento, 26, **7-8** (2003).
[5] Y. Kubota *et al.*, Nucl. Instrum. Meth. Phys. Res., Sect. A **320**, 66 (1992); D. Peterson *et al.*, Nucl. Instrum. Meth. Phys. Res., Sect. A **478**, 142 (2002); M. Artuso *et al.*, Nucl. Instrum. Meth. Phys. Res., Sect. A **554**, 147 (2005).
[6] R. E. Mitchell *et al.* (CLEO Collaboration), Phys. Rev. Lett. **102**, 081801 (2009).
[7] D. Besson *et al.* (CLEO Collaboration), Phys. Rev. D **80**, 032005 (2009).
[8] S. Dobbs *et al.* (CLEO Collaboration), Phys. Rev. D **76**, 112001 (2007).
[9] C. Amsler *et al.* (Particle Data Group), Review of Particle Physics, Phys. Lett. B **667**, 1 (2008).
[10] R. Gray, Ph.D. thesis, Cornell University, 2008.
[11] D. Cronin-Hennessey *et al.* (CLEO Collaboration), Phys. Rev. Lett. **100**, 251802 (2008), and S. Dobbs *et al.*, (CLEO Collaboration), Phys. Rev. D **77**, 112005 (2008).
[12] R. Brun *et al.*, `GEANT 3.21`, CERN Program Library Long Writeup W5013, unpublished.
[13] D. J. Lange, Nucl. Instrum. Meth. A **462** (2001) 152.
[14] T. Skwarnicki, Ph.D thesis, Jagiellonian University in Krakow, 1986, DESY Report No. F31-86-02.
[15] See EPAPS Document No. [X] for covariance matrices and alternate $f_+(q^2$ fits. For more information on EPAPS, see http://www.aip.org/pubservs/epaps.html.
[16] T. Becher and R.J. Hill, Phys. Lett. B **633**, 61 (2006). R. J. Hill, *The Proceedings of 4th Flavor Physics and CP Violation Conference*, Vancouver, BC, Canada, 9-12 Apr 2006, pp 027; *The Proceedings of International Workshop on Charm Physics*, Ithaca, NY, 5-8 Aug 2007, pp 22.
[17] S. Fajfer and J. Kamenik, Phys. Rev. D **71**, 014020 (2005).